JOURNAL OF VIROLOGY, Feb. 2005, p. 2440–2448 Vol. 79, No. 4
0022-538X/05/$08.00+0 doi:10.1128/JVI.79.4.2440–2448.2005

Characterization of Helper Virus-Independent Cytopathogenic Classical Swine Fever Virus Generated by an In Vivo RNA Recombination System

Andreas Gallei, Till Rümenapf, Heinz-Jürgen Thiel, and Paul Becher*

Institut für Virologie, Justus-Liebig-Universität, Giessen, Germany

Received 1 July 2004/Accepted 28 September 2004

Molecular analyses revealed that most cytopathogenic (cp) pestivirus strains evolve from noncytopathogenic (noncp) viruses by nonhomologous RNA recombination. In contrast to bovine viral diarrhea virus (BVDV), cp classical swine fever virus (CSFV) field isolates were rarely detected and always represented helper virus-dependent subgenomes. To investigate RNA recombination in more detail, we recently established an in vivo system allowing the efficient generation of recombinant cp BVDV strains in cell culture after transfecting a synthetic subgenomic and nonreplicatable transcript into cells being infected with noncp BVDV (A. Gallei, A. Pankraz, H.-J. Thiel, and P. Becher, J. Virol. 78:6271–6281, 2004). Using an analogous approach, the first helper virus-independent cp CSFV strain (CP G1) has now been generated by RNA recombination. Accordingly, this study demonstrates the applicability of RNA recombination for designing new viral RNA genomes. The genomic RNA of CP G1 has a calculated size of 18.139 kb, almost 6 kb larger than all previously described CSFV genomes. It contains cellular sequences encoding a polyubiquitin fragment directly upstream of the nonstructural protein NS3 coding gene together with a duplication of viral sequences. CP G1 induces a cytopathic effect on different tissue culture cell lines from pigs and cattle. Subsequent analyses addressed growth kinetics, expression of NS3, and genetic stability of CP G1.

Classical swine fever virus (CSFV), the causative agent of an economically important disease in pigs, forms together with the species *Bovine viral diarrhea virus* 1 (BVDV-1), BVDV-2, and *Border disease virus* (BDV) the genus *Pestivirus*, family *Flaviviridae* (11, 22). Highly virulent CSFV strains can cause a severe form of classical swine fever, characterized by pyrexia; hemorrhages in the skin, mucosa, and inner organs; anorexia; diarrhea; and, in late stages, central nervous disorders resulting in high morbidity and mortality (48). However, most CSFV strains isolated from recent outbreaks in Europe led to chronic forms of disease with less characteristic symptoms (16).

Pestiviruses are small enveloped viruses encompassing a single-stranded RNA genome of positive polarity with a length of about 12.3 kb. The viral genomic RNA is neither capped nor polyadenylated and contains one large open reading frame (ORF) flanked by 5′ and 3′ nontranslated regions (NTR); the latter harbor *cis*-active elements essential for viral translation and replication. The ORF encodes a polyprotein of approximately 3,900 amino acids (aa) that is co- and posttranslationally processed by cellular and viral proteases to the mature viral proteins (22, 29, 36, 48).

For pestiviruses, cytopathogenic (cp) and noncytopathogenic (noncp) strains are distinguished by their ability to cause a cytopathic effect (CPE) in susceptible tissue culture cells (18, 28). For BVDV it is well documented that cp strains mostly evolve by nonhomologous RNA recombination in animals persistently infected with noncp BVDV. The emergence of cp BVDV in persistently infected animals is crucial for the induction of lethal mucosal disease in cattle (13, 14). Molecular analyses of cp BVDV and cp BDV strains led to detection of various genomic alterations, including insertions of cellular mRNA sequences as well as duplications and deletions of viral sequences (4–6, 8, 31, 32, 47).

In contrast to BVDV, cp CSFV strains were rarely identified (15, 19, 27, 49). Interestingly, all cp CSFV field isolates analyzed so far consist of a noncp CSFV strain together with a viral subgenome. With the exception of subgenome cpBW1, which lacks 4,746 nucleotides (nt) (24), all other subgenomes are characterized by a common internal deletion of 4,764 nt, resulting in fusion of the translation initiation codon to the first codon of the NS3 gene (1, 24, 35). It could be demonstrated that the deletion of these CSFV subgenomes represents the genetic basis for expression of large amounts of NS3 and cytopathogenicity. The respective subgenomes are defective interfering particles (DI) dependent on the presence of a helper virus for packaging (37). Such strains were isolated not only from domestic pig and wild boar but also from tissue culture cells in which noncp CSFV was passaged (1, 35, 39).

To study various aspects of RNA recombination, we recently established the first in vivo RNA recombination system for pestiviruses which allowed the efficient generation of cp BVDV strains in cell culture (17). Here, we report on an analogous approach for CSFV. The obtained CSFV strain CP G1 represents the first helper virus-independent cp CSFV that originated from RNA recombination. This study demonstrates the applicability of RNA recombination for the design of new RNA viruses with a desired phenotype.

MATERIALS AND METHODS

Cells and viruses. Madin-Darby bovine kidney (MDBK) cells as well as porcine kidney (PK15) cells were obtained from the American Type Culture Collection (Manassas, Va.). Swine kidney (SK6) cells were a kind gift of J. D.

* Corresponding author. Mailing address: Institut für Virologie, Justus-Liebig-Universität, Giessen, Germany. Phone: 49-641-99-38376. Fax: 49-641-99-38359. E-mail: Paul.Becher@vetmed.uni-giessen.de.

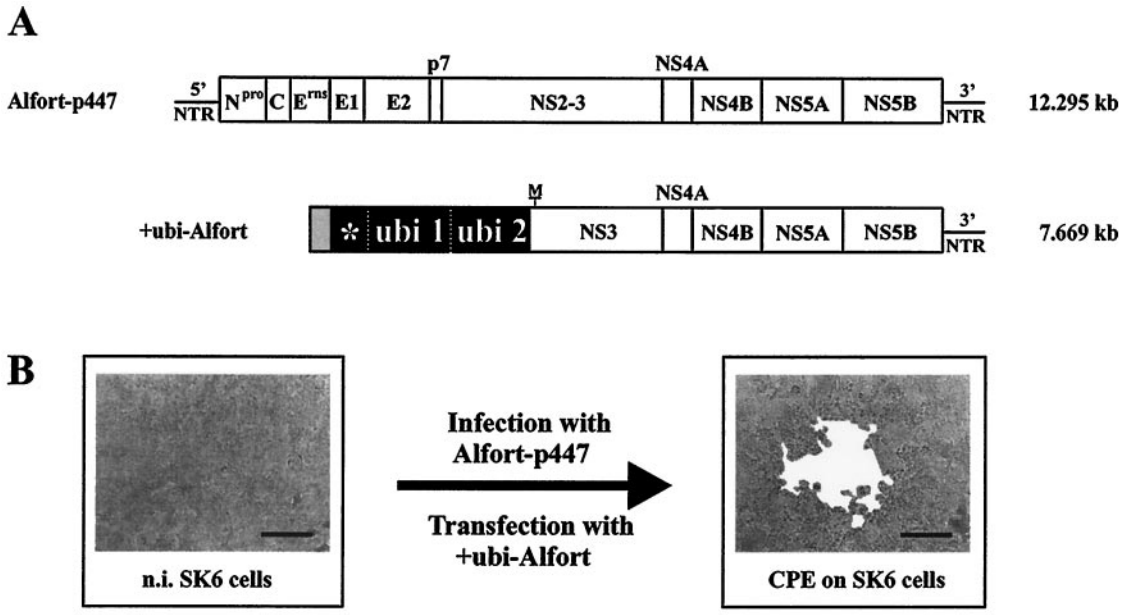

FIG. 1. In vivo RNA recombination system for CSFV. (A) Schematic representation of the recombination partners. The top schematic shows the RNA genome of noncp CSFV strain Alfort-p447 containing one large ORF (box) flanked by 5′ and 3′ NTRs. The positions of the genes encoding the viral structural proteins (capsid protein C and envelope proteins E^{rns}, E1, and E2) and nonstructural (NS) proteins (N^{pro}, p7, NS2-3, NS4A, NS4B, NS5A, and NS5B) are indicated. The bottom schematic shows genome organization of the synthetic, replication-incompetent transcript +ubi-Alfort encoding the C-terminal five amino acids of NS2 of BVDV strain CP14 (grey box) and a C-terminal fragment (marked by an asterisk) as well as two complete monomers of cellular ubiquitin (ubi 1 and ubi 2) followed by viral proteins NS3, NS4A, NS4B, NS5A, and NS5B derived from noncp CSFV strain Alfort-p447. The transcript +ubi-Alfort also comprises the 3′ NTR but lacks the entire 5′ NTR and, thereby, *cis*-acting signals essential for translation and replication. An ApaI site (M) was introduced as a genetic marker for +ubi-Alfort-derived sequences. The bars are not drawn to scale. The sizes of Alfort-p447 and +ubi-Alfort are indicated in kilobases (kb) on the right. (B) Noninfected (n.i.) SK6 cells (left) and SK6 cells 24 h after infection with supernatant obtained from cells previously infected with Alfort-p447 that showed a CPE 5 days after transfection with +ubi-Alfort (right). The area of lysed cells is white. Scale bar, 200 μm.

Tratschin, Institute of Virology and Immunoprophylaxis, Mittelhäusern, Switzerland. Cells were grown in Dulbecco's modified Eagle's medium supplemented with 10% horse serum. noncp CSFV strain Alfort-p447 (Fig. 1A) was derived from infectious cDNA clone pAlfort-p447 (see below).

Infection of cells, immunofluorescence, crystal violet staining of cells, and determination of growth kinetics. Supernatants of infected cells were used for further infections. Material for infections was harvested 48 to 72 h postinfection and stored at −70°C. With respect to all cell culture passages of cp CSFV, complete lysis of cells occurred at 24 to 36 h postinfection (hpi). As one pestiviral replication cycle is completed within about 10 h, it can be assumed that each passage comprises approximately two to three viral replication cycles. Infection with noncp CSFV was detected by indirect immunofluorescence (IF) with monoclonal antibody A18 directed against glycoprotein E2 (50). Crystal violet staining of cells and determination of growth kinetics have been described elsewhere (7, 12).

Construction of cDNA clones. Nucleotide numbers throughout this study refer to the sequence of CSFV Alfort/Tü, GenBank accession number J04358 (30). The infectious full-length CSFV cDNA clone pAlfort-p447 is a modified version of pA/CSFV (30) which has a vector backbone derived from pBR322 (instead of pACYC177). Further modifications include the introduction of an SP6 promoter and silent mutations of internal SmaI sites, leaving a unique SmaI site at the 3′ end for linearization of template DNA. Repair of a frameshift due to a missing C residue at position 7907 in pA/CSFV resulted in a 1,000-fold increased specific infectivity exceeding 10^6 focus-forming units per μg of RNA after transfection into PK15 cells. For construction of p+ubi-Alfort, the XhoI (214)/EcoRI (5560) fragment of pAlfort-p447 was replaced by a corresponding XhoI/EcoRI fragment. The latter encompasses a T7 promoter downstream of its XhoI site followed by a cDNA sequence derived from BVDV strain CP14 that encodes the C-terminal 5 amino acids (aa) of NS2 as well as a C-terminal fragment and two complete monomers of cellular ubiquitin (46). This sequence is followed by the 5′-terminal part of the NS3 gene derived from pAlfort-p447, including its singular EcoRI (5560) site. Due to cloning procedures, nucleotide (nt) 5145 of pAlfort-p447 was changed from A to C. This silent mutation generated an ApaI site serving as a genetic marker (M) for +ubi-Alfort-derived sequences (Fig. 1A).

In vitro synthesis of RNA. After complete digestion of plasmid p+ubi-Alfort with SmaI, linearized DNA was extracted with phenol-chloroform and precipitated with ethanol. RNA was transcribed by use of T7 RNA-dependent RNA polymerase (Ambion) using standard conditions. The quality and amount of RNA were controlled by ethidium bromide staining after agarose gel electrophoresis. The RNA transcript used for transfection contained >80% of intact RNA.

Transfection of RNA and isolation of recombinant cp CSFV. For transfection, the confluent SK6 cells from a dish 10 cm in diameter that were previously infected with noncp CSFV Alfort-p447 were trypsinized, resuspended in 0.4 ml of phosphate-buffered saline (PBS) without Ca^{2+} and Mg^{2+}, and mixed with in vitro-transcribed +ubi-Alfort RNA immediately before the pulse (950 μF and 180 V). For electroporation, a Gene Pulser II (Bio-Rad, Munich, Germany) was used. The electroporated cells were distributed to 24 wells of two 12-well plates immediately posttransfection and were adjusted to 2 ml with medium for each well; 5 days posttransfection, the cells of each well were trypsinized, resuspended, and transferred separately to a well of a 6-well plate. After additional incubation for 24 h, the cells were monitored by microscopical inspection. After the appearance of a CPE, the respective supernatant and cellular RNA were harvested. For control, noninfected (n.i.) cells and cells infected with Alfort-p447 were electroporated without +ubi-Alfort RNA. Moreover, n.i. cells were also transfected with +ubi-Alfort RNA. Respective cells were seeded in 6-well plates immediately posttransfection and checked 1 and 5 days posttransfection by light microscopy and IF analysis for emergence of a CPE and expression of viral proteins, respectively.

RNA preparation, Northern (RNA) hybridization, RT-PCR, molecular cloning, and nucleotide sequencing. Methods for RNA preparation, Northern hybridization, reverse transcription-PCR (RT-PCR), molecular cloning, and nucleotide sequencing have been described previously (6). The following primer pairs were used in RT-PCR as described below in Results. Primer pair 1, Ol Alfort-10033 (5′-CACATATGGTCTCAGCCTACC-3′; nt 10013 to 10033) and Ol Al-

fort-5153R (5′-GTGTTCAGTAACCTTCTTGC-3′; nt 5153 to 5172); primer pair 2, Ol Alfort-10033 and Ol Alfort-5672R (5′-GTTCTTCCCGACCTTGAC CC-3′; nt 5672 to 5691); primer pair 3, Ol Alfort-7017 (5′-TGGAGAGGTGA CTGATACTTAC-3′; nt 6996 to 7017) and Ol Alfort-5153R; primer pair 4, Ol Alfort-191 (5′-GTACAGGACAGTCGTCAGTAG-3′; nt 171 to 191) and Ol Alfort-6017R (5′-AAGTAACCGTAAGAGGCATAGG-3′; nt 6017 to 6038).

Immunoblot analysis. Immunoblot analysis was performed essentially as previously described (6, 45). For CP G1, the sample was obtained from the third cell culture passage.

RESULTS

Establishment of an in vivo RNA recombination system for CSFV. An efficient in vivo RNA recombination system has recently been established which allows the generation of recombinant cp BVDV strains (17). This system is based on the transfection of synthetic, subgenomic, and nonreplicatable transcript +ubi SGT into cells infected with noncp BVDV NCP7. +ubi SGT encodes the C′-terminal 5 aa of nonstructural protein 2 (NS2) of BVDV strain CP14, a C-terminal fragment and two complete copies of cellular ubiquitin, and viral NS3, NS4A, NS4B, NS5A, and NS5B of noncp BVDV strain NCP7. It also comprises the 3′-nontranslated region (NTR) but lacks the entire 5′ NTR with *cis*-acting signals essential for translation and replication as well as the genomic region encoding the NS proteins N^{pro}, p7, and NS2 and the structural proteins. Molecular analyses of 46 resulting different cp BVDV recombinants revealed that each one originated from a single nonhomologous recombination event that occurred in frame between the replicating noncp BVDV NCP7 genome and the 5′ part of +ubi SGT (17). In order to apply the system to a different pestivirus, our assay was adapted to CSFV by generation of transcript +ubi-Alfort. In analogy to +ubi SGT, the latter encodes the C′-terminal 5 aa of NS2 of BVDV strain CP14 followed by a C′-terminal fragment and two complete copies of cellular ubiquitin. These BVDV CP14-derived sequences (46) are followed by CSFV Alfort-p447-specific sequences that encode proteins NS3 to NS5B and also include the viral 3′ NTR. Accordingly, +ubi-Alfort lacks the entire 5′ NTR with *cis*-acting signals essential for translation and replication as well as the genomic region encoding the structural proteins and the NS proteins N^{pro}, p7, and NS2 (Fig. 1A). Studies performed with BVDV showed that the highest number of recombinants was obtained with the largest amount (10 μg) of transcript +ubi SGT (17 and data not shown). The correlation between recombination frequency and the amount of transcript will be addressed in a future study. Accordingly, in one experiment, 2.5×10^7 porcine SK6 cells previously infected with noncp CSFV Alfort-p447 were transfected by electroporation with about 10 μg of +ubi-Alfort RNA and seeded into 24 wells of two 12-well dishes. Five days posttransfection, cells of each well were separately transferred onto one well of four 6-well cell culture dishes. In one well of these 6-well dishes, several dozens of plaques rapidly emerged after an additional incubation period of 24 h. Moreover, after 48 h of incubation, 19 additional wells showed a CPE. For the latter, a detailed analysis will be presented in a separate study. For further investigation, only the supernatant of cells showing a CPE already after 24 h was used for infection of noninfected (n.i.) SK6 cells. At 24 hpi, a clear CPE could be again observed (Fig. 1B), and both total RNA (CPE-P1) and supernatant of this first cell culture passage were prepared.

Control experiments including (i) electroporation of n.i. cells without transfecting +ubi-Alfort RNA, (ii) transfection of +ubi-Alfort RNA into n.i. cells, or (iii) electroporation of cells previously infected with Alfort-p447 in the absence of +ubi-Alfort RNA did not lead to a CPE (data not shown). For these controls, the same number of cells and amount of synthetic transcript were used. Presence of viral antigen was demonstrated by IF analysis in cells infected with Alfort-p447 but not in n.i. cells (data not shown).

Biological cloning and genome analysis of recombinant cp CSFV. Detection of a CPE after transfection of +ubi-Alfort RNA into cells infected with noncp CSFV Alfort-p447 led to the assumption that a replication-competent, recombinant cp CSFV was generated. To separate the putative recombinant cp CSFV strain from noncp strain Alfort-p447, an at least threefold plaque purification of seven independently picked plaques was performed on SK6 cells. After this procedure, total RNA derived from the first cell culture passage was analyzed by Northern blot hybridization. For each sample, a single RNA with a size of about 18 kb was detected, demonstrating the presence of a significantly enlarged pestiviral genome. There was no evidence for the presence of the genome of Alfort-p447 or additional viral (sub)genomic RNAs (data not shown) (Fig. 2A). In the following investigation, one of these seven biologically cloned cp CSFV strains (termed CP G1) was randomly selected for further analyses.

To determine the genome organization of CP G1, RNA used for Northern blot analysis was subjected to RT-PCR analysis using different pairs of primers (see Materials and Methods). By use of primer pair 1, a specific product indicating the presence of duplicated viral sequences was obtained. Subsequent cloning and nucleotide sequencing led to identification of a recombinant sequence which resulted from nonhomologous RNA recombination between the genome of Alfort-p447 and +ubi-Alfort (Fig. 2B). The deduced genome organization of CP G1 comprises a unique duplication of viral sequences together with an insertion of ubiquitin-encoding sequences. The enlarged genome maintains the ORF and consists of nucleotides 1 to 10470 of Alfort-p447 followed by a complete version of +ubi-Alfort. The calculated total genomic size of CP G1 is 18.139 kb and is thus about 1.5 times larger than that of all CSFV genomes described before. This size corresponds to the enlarged viral genomic RNA detected by Northern blot analysis (Fig. 2A and C). In addition, CPE-P1 RNA was subjected to RT-PCR analysis by use of primer pair 2. A specific product was cloned and sequenced. The obtained nucleotide sequence showed that the genome of CP G1 was already present before plaque purification (data not shown).

By use of various primer pairs, RT-PCR analyses of the RNA derived from the first cell culture passage of biologically cloned CP G1 did not indicate the presence of additional CSFV-specific RNAs (data not shown). The ability of CP G1 to induce a CPE on SK6 cells was demonstrated by subsequent cell culture passages (Fig. 2D).

Further characterization of CP G1. To investigate whether CSFV CP G1 is able to cause a CPE on cell lines other than SK6, infections were performed using porcine PK15 as well as bovine MDBK cells. Cells were infected with supernatant from

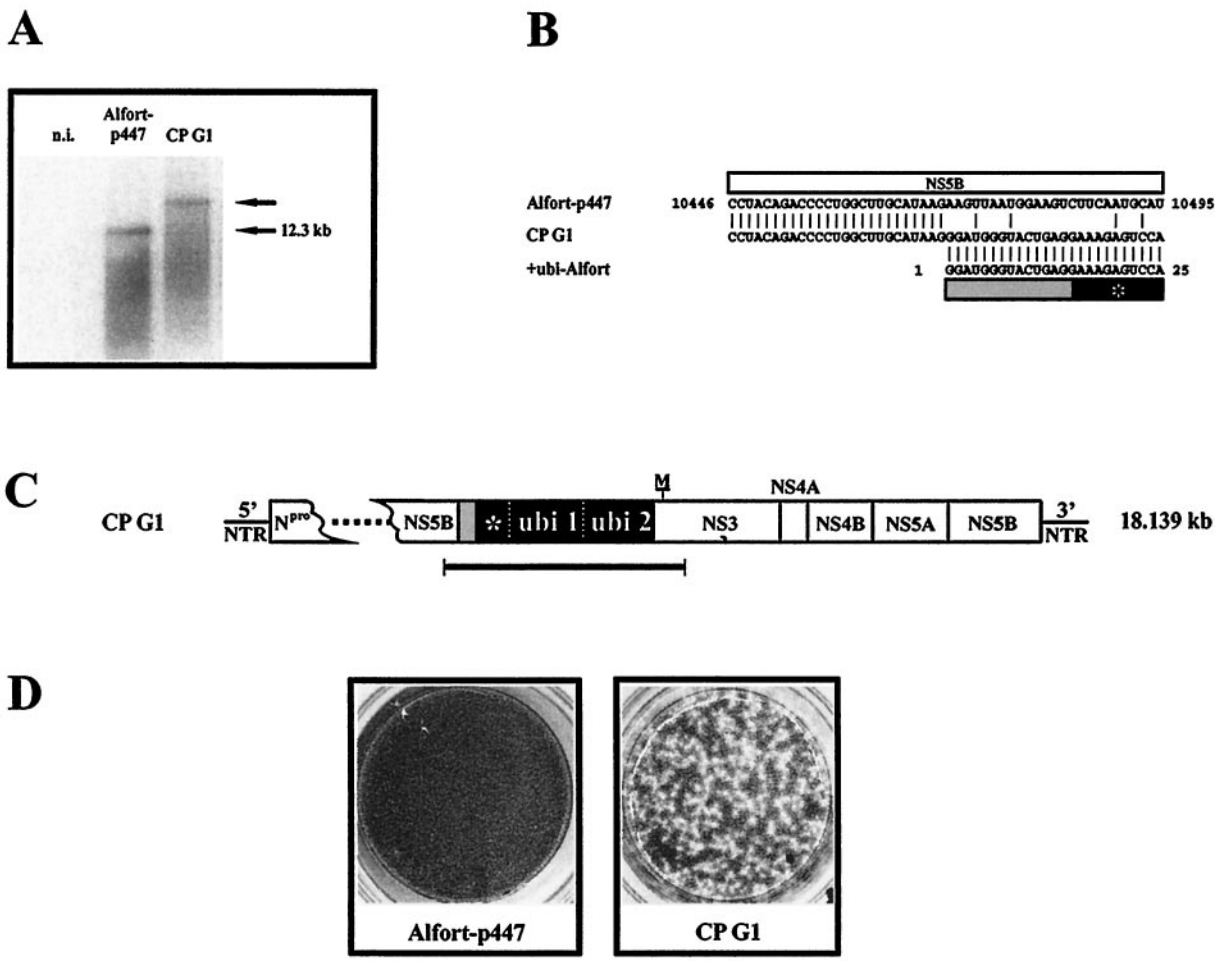

FIG. 2. Analysis of CSFV recombinant CP G1. (A) Northern blot analysis of total RNA from noninfected (n.i.) SK6 cells, cells infected with Alfort-p447, and the first cell culture passage of biologically cloned CSFV strain CP G1. For hybridization, a radioactively labeled EcoRI/NaeI cDNA fragment corresponding to nt 5560 to 8340 of Alfort-p447 was used. The size of Alfort-p447 RNA (in kilobases) and migration positions of apparent viral genomic RNAs of Alfort-p447 and CP G1 are indicated on the right. Note the enlarged genome of CP G1. (B) Alignment of sequences in the crossover region of CSFV CP G1. Nucleotide sequences of the parental RNAs Alfort-p447 and +ubi-Alfort (upper and lower lines, respectively) are shown together with the sequence of the obtained recombinant CSFV strain CP G1 (middle line). Sequence identities between recombinant and parental RNAs are indicated by vertical lines. The bars above and below the alignment indicate the genomic positions of the parental sequences. (C) Genome organization of CSFV strain CP G1 that resulted from RNA recombination between Alfort-p447 and +ubi-Alfort. The region between the N^{pro} gene and the 5′-terminal part of the NS5B gene is indicated by dots. The recombinant RNA contains a complete copy of +ubi-Alfort fused to nt 10470 of the genome of Alfort-p447. The underlined part of the genome has been sequenced. The genetic marker M (ApaI site) indicates the presence of +ubi-Alfort-derived sequences. The calculated length of the genome is shown in kilobases on the right. Bar lengths are not drawn to scale. (D) Crystal violet staining of SK6 cells infected with noncp CSFV Alfort-p447 (left) and CP G1 (right). For the latter, the second cell culture passage was used. After infection, the cells were overlaid with medium containing 0.6% low-melting-point agarose. After incubation for 4 days, the cells were fixed and stained. Note the CPE caused by infection with CP G1 in contrast to that of cells infected with noncp CSFV Alfort-p447.

the first cell culture passage of CP G1 or with noncp CSFV Alfort-p447. With respect to infection with CP G1, lysis of cells was observed not only for SK6 cells but also for PK15 and MDBK cells (Fig. 3). The occurrence of a CPE correlated with detection of viral antigen by IF analysis (data not shown). Infection of bovine MDBK cells with CP G1 resulted in a considerably lower amount of plaques (data not shown) that were significantly smaller than the ones produced in porcine SK6 and PK15 cells (Fig. 3). These observations confirm previously reported findings that bovine cells are less susceptible to infection with CSFV than porcine cells (43). In contrast to cells infected with CP G1, cells infected with noncp CSFV Alfort-p447 showed no signs of a CPE (Fig. 3).

For further characterization, the growth rate and yield of CP G1 were determined using SK6 cells infected at a multiplicity of infection (MOI) of 0.3. Virus released into the medium was counted over a 3-day period. Infectious virus titers determined by light microscopy and IF analysis were identical. The peak titer of CP G1 reached at 36 hpi was 1.3×10^7 50% tissue culture infectious doses/ml. At later time points the titers decreased slightly, probably due to progressing cell lysis. For comparison, the growth kinetic of the parental noncp CSFV

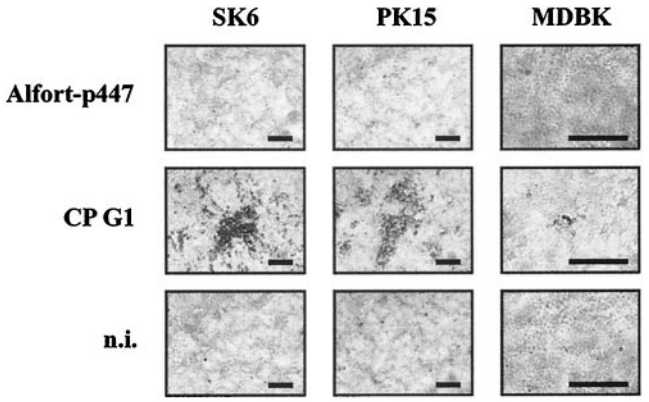

FIG. 3. Growth properties of CP G1 in different cell lines. Porcine SK6 (left) and PK15 cells (middle) as well as bovine MDBK cells (right) were infected with noncp CSFV Alfort-p447 (top) or CP G1 from the first cell culture passage (middle). Noninfected (n.i.) cells (bottom) served as negative controls. After infection, only porcine cells were overlaid with medium containing 0.6% low-melting-point agarose. After an incubation period of 66 h at 37°C, a CPE was only observed after infection with CSFV CP G1. Scale bar, 200 μm.

strain Alfort-p447 was determined using the same MOI. Here, the peak titer of 2.3×10^7 50% tissue culture infectious doses /ml was reached at 43 hpi. While the relative fitness of CP G1 and Alfort-p447 remains to be investigated, both viruses show very similar growth kinetics until 36 hpi (Fig. 4A).

Cytopathogenicity of pestiviruses, including CSFV, has been demonstrated to correlate with the expression of large amounts of NS3, the C-terminal part of NS2-3 (3, 5, 8, 34, 35, 46, 47). The genetic basis for strong expression of NS3 and viral cytopathogenicity has been demonstrated for various pestiviral strains (4, 9, 12, 25, 32, 33, 37, 40). For pestiviral genomes with ubiquitin-encoding sequences directly upstream of the NS3 gene, it has been shown that ubiquitin provides an additional cleavage site for cellular proteases within the viral polyprotein. This processing event leads to efficient release of NS3 (46). In contrast to noncp BVDV, where NS3 is usually no more detectable at late phases of infection (26), a minimal expression of NS3 has been reported to occur after infection with noncp BDV and noncp CSFV (10, 35). To study expression of NS3 and uncleaved NS2-3 in cells infected with cp CSFV CP G1, an immunoblot was performed. As expected, these analyses demonstrated a large amount of NS3 (Fig. 4B). A considerably smaller amount of NS3 was detected after infection with noncp CSFV Alfort-p447, while similar amounts of uncleaved NS2-3 were found after infection with both cp CSFV CP G1 and noncp CSFV Alfort-p447 (Fig. 4B).

Genetic stability of CP G1. It has been described previously that cp BVDV genomes carrying duplications of viral sequences can undergo secondary genetic changes by RNA recombination resulting in various deletions. As a consequence of such events, the emergence of noncp viruses or viral subgenomes during cell culture passages has been reported (4, 9). Accordingly, it was interesting to examine the genetic stability of CP G1. The possible emergence of noncp CSFV during cell culture propagation was monitored by IF analysis of cells infected with CP G1. After 10 cell culture passages, IF analysis did not indicate the presence of noncp virus (data not shown).

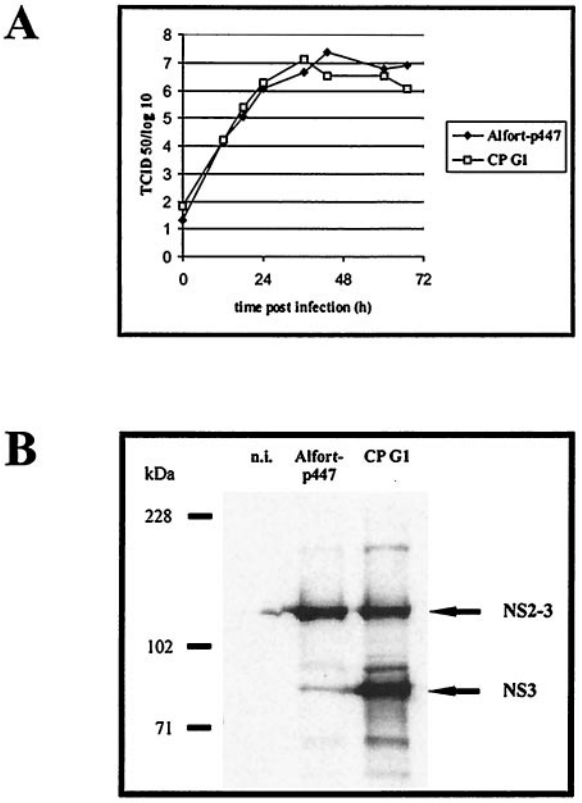

FIG. 4. Growth kinetics and expression of NS2-3 and NS3 after infection with CSFV strains CP G1 and Alfort-p447. (A) Growth curves of cp CSFV CP G1 and noncp CSFV Alfort-p447 determined on SK6 cells infected at a multiplicity of infection (MOI) of 0.3. The titers of released virus were determined at the indicated time points over a 3-day period. (B) Immunoblot analysis of SK6 cells infected with CP G1 or Alfort-p447 at an MOI of 0.3. Cells were lysed 24 hpi. The samples were subjected to sodium dodecyl sulfate-polyacrylamide gel electrophoresis under reducing conditions, transferred to a nitrocellulose membrane, and analyzed by using an anti-NS3 monoclonal antibody. Note the large amount of NS3 derived from cells infected with CP G1. Marker proteins are indicated in kilodaltons (kDa) on the left. The positions of NS2-3 and NS3 are marked with arrows. n.i., noninfected SK6 cells.

In addition, total cellular RNA derived from the 10th passage of CP G1 (CP G1-P10) was subjected to Northern blot analysis. Surprisingly, a viral genomic RNA of about 15 kb was detected, considerably shorter than the CP G1 RNA from the first passage. In addition, a broad subgenomic band was detected (Fig. 5A).

For further characterization, CP G1-P10 RNA was subjected to RT-PCR analysis using a set of primer pairs (see Materials and Methods). By use of primer pair 2, a specific product indicating the presence of the genome of CP G1 was not detectable (data not shown). In contrast, RT-PCR analysis with primer pair 3 resulted in a specific product that was subsequently cloned and sequenced. According to comparative sequence analysis, sequences that encode NS4B were fused to sequences correlating to the 3′ part of the CP G1 genome encoding polyubiquitin (Fig. 5B). The calculated size of the recombinant genome that maintains the ORF is 14.980 kb and corresponds to the viral genomic RNA detected by Northern

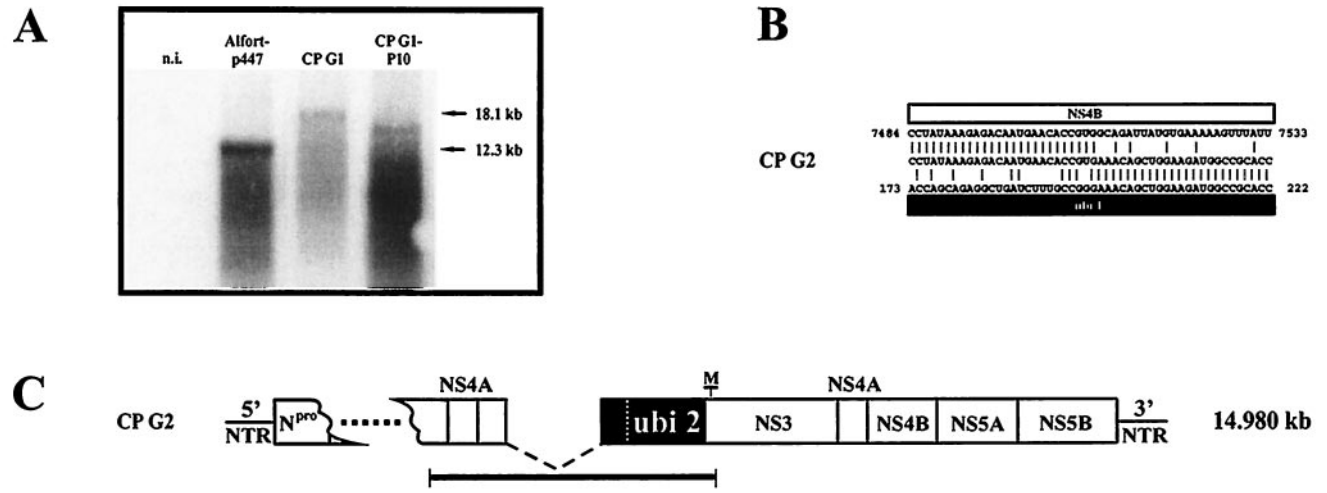

FIG. 5. Genetic stability of CP G1. (A) Northern blot analysis of total RNA from noninfected (n.i.) SK6 cells and SK6 cells infected with noncp CSFV Alfort-p447 as well as cp CSFV CP G1 from the 1st (CP G1) and 10th cell culture passage (CP G1-P10). For hybridization, a radioactively labeled EcoRI/NaeI cDNA fragment of pAlfort-p447 was used. Migration positions and sizes of the viral genomic RNAs of Alfort-p447 and CP G1 are indicated in kilobases on the right. For CP G1-P10, note presence of a viral genomic RNA of about 15 kb in length as well as the presence of subgenomic RNAs. (B) Alignment of sequences in the crossover region of CSFV CP G2. The parental sequences derived from CP G1 that encode part of NS4B (top) or ubi 1 (bottom) are compared to the recombinant sequence of CSFV CP G2 (middle line). Sequence identities between recombinant and parental RNAs are indicated by vertical lines. The genomic positions of the parental sequences are shown as bars above and below the alignment. Numbers flanking the parental sequences refer to the genome of CSFV CP G1 (top) and +ubi-Alfort (bottom). (C) Genome organization of CSFV strain CP G2. The region between the N^{pro} gene and the 5′-terminal NS4A gene is partially indicated by dots. At its 5′ part the recombinant RNA consists of sequences corresponding to a 3′-truncated genome of CP G1 (left) fused to sequences correlating to the 3′ part of the CP G1 genome (right). Respective parts of the CP G2 genome are connected by dashed lines. The underlined part of the genome has been sequenced. M, genetic marker (see also Fig. 2C). The calculated length of the genome is shown in kilobases on the right. Bar lengths are not drawn to scale.

blot analysis (Fig. 5A and C); this recombinant genome is termed CP G2.

To characterize the broad subgenomic band detected by Northern blot analysis of CP G1-P10 RNA, primer pair 4 was used for RT-PCR analysis. Several specific products were obtained, suggesting the presence of a variety of viral subgenomic RNAs. In contrast, specific products were not obtained by RT-PCR performed with RNA from n.i. cells or from cells infected with either noncp CSFV Alfort-p447 or the first cell culture passage of biologically cloned cp CSFV strain CP G1 (data not shown). Molecular cloning and nucleotide sequencing of the specific RT-PCR products led to identification of recombinant CSFV subgenomes 1 to 12, resulting from fusion of sequences corresponding to the 5′ part of the CP G1 genome (encoding N^{pro} or C) to sequences corresponding to the BVDV CP14-specific part of CP G1. For all subgenomes the ORF was maintained. All subgenomes carry unique crossover sites and encode at least one complete ubiquitin monomer directly followed by NS3. The calculated sizes of the subgenomes range between 7.888 and 8.596 kb (Fig. 6). Moreover, it cannot be excluded that additional subgenomes were present. According to previous studies on pestiviral subgenomes, the 12 CSFV subgenomes are expected to be helper virus dependent (9, 37, 39). Taken together, passages of CP G1 in cell culture led to various genomic deletions, resulting in the emergence of a viral genomic RNA with a length of 14.980 kb (CP G2) together with at least 12 unique viral subgenomes.

To determine whether subgenomes were present earlier, an RT-PCR analysis specific for subgenomes was performed that included RNAs from the first cell culture passage of CP G1 and from cells infected with supernatants from the first to ninth cell culture passage of CP G1 (RNAs P2-P10). Specific products indicating the presence of subgenomes were obtained for RNA P2-P10 but not for RNA prepared from the first passage of CP G1 (data not shown). This suggests that the CSFV subgenomes had already evolved during the second cell culture passage.

To investigate the genetic stability of CP G2, five independently picked plaques (obtained from the 11th cell culture passage of CP G1) were subjected to threefold plaque purification and subsequently passaged. Again, the cp phenotype was retained. RT-PCR and Northern blot analyses of RNAs from the 11th cell culture passage demonstrated for three of the five samples the presence of a viral genomic RNA corresponding in size to the genome of CP G2 as well as various viral subgenomes with a length of about 7.5 to 8.5 kb; in the other two samples, the CP G2 RNA was replaced by a viral genomic RNA with a length of about 14.0 to 14.5 kb; subgenomic RNAs were also present (data not shown). Similar to CP G1, CP G2 represents a helper virus-independent cp CSFV which is not genetically stable during cell culture propagation.

DISCUSSION

The existence of two biotypes, namely cp and noncp viruses, represents a remarkable feature of pestiviruses. The biological significance and molecular aspects of cytopathogenicity have been extensively studied for BVDV, and a large number of cp BVDV strains carrying a variety of genomic alterations have been characterized. In contrast to BVDV, only a few cp CSFV

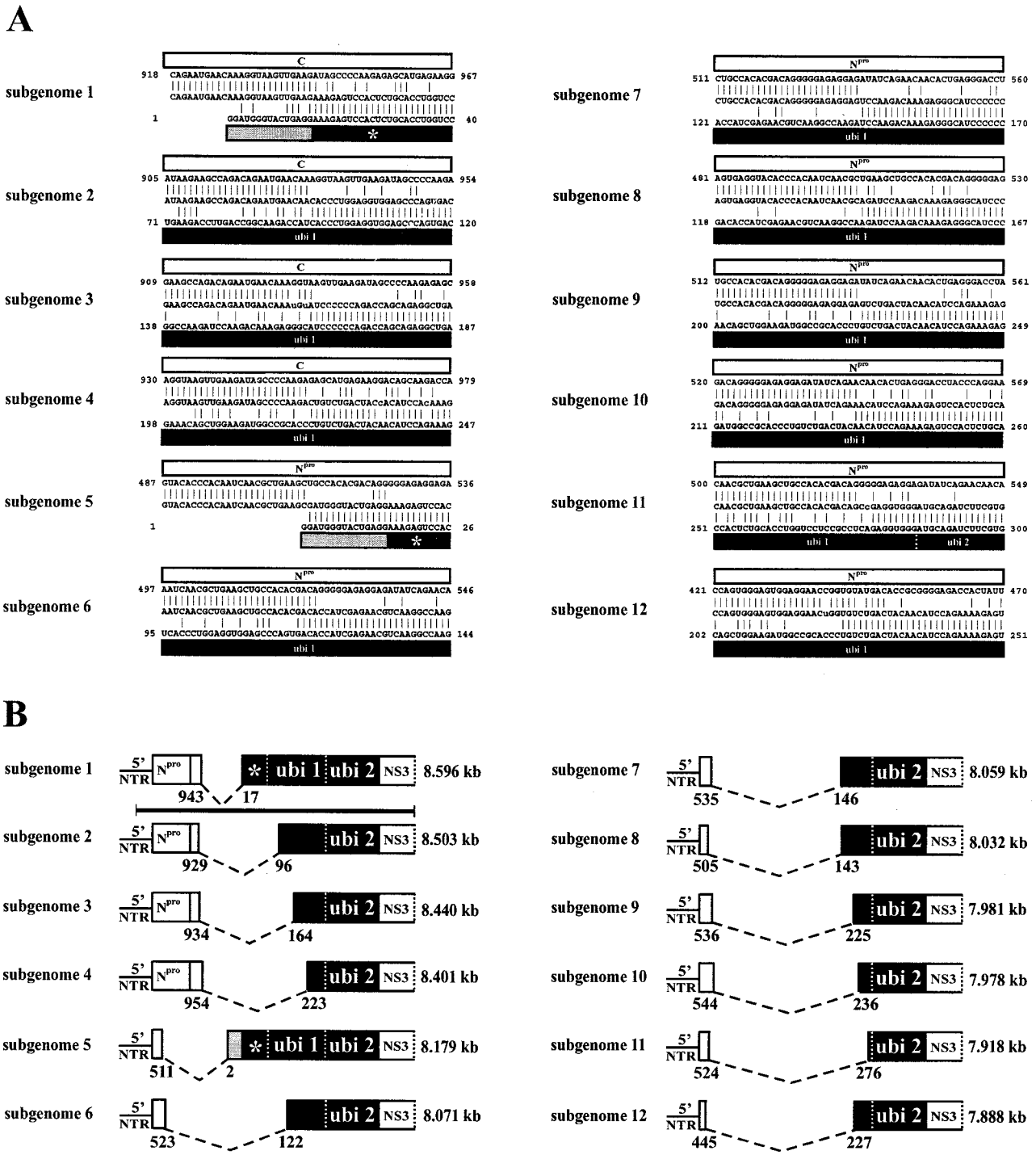

FIG. 6. Crossover regions and genome organization of recombinant CSFV subgenomes 1 to 12. (A) Alignment of sequences in the crossover regions. The parental sequences that correspond to various regions of the genes encoding N^{pro} or C (top) and to the BVDV CP14-derived part (bottom) of the CP G1 genome are compared to sequences of the obtained recombinant CSFV subgenomes 1 to 12 (middle line), respectively. Sequence identities between recombinant and parental RNAs are indicated by vertical lines. Nucleotide sequence differences between the recombinant and parental sequences are indicated by lowercase letters. The genomic positions of the parental sequences are shown as bars above and below the alignment. Numbers flanking the parental sequences refer to the genome of CSFV CP G1 (top) and +ubi-Alfort (bottom), respectively. (B) Genome organization and calculated sizes of CSFV subgenomes 1 to 12. Respective parts of the genomes are connected by dashed lines. The regions downstream of the 5′-terminal part of the NS3 gene are not included. Numbers below the recombinant genomes indicate the positions of the 5′ and 3′ junction sites and refer to the genome of CP G1 (left) and to +ubi-Alfort (right). In the case of local sequence identity between parental sequences at the recombination site (see panel A, for example subgenome 1), the numbers were calculated by assuming a maximum integration of the 5′ sequence. As indicated for subgenome 1 by a line below the genome, the genomic regions between the viral 5′ NTR and the 5′ part of the NS3 gene have been sequenced for all subgenomes. All recombinants carry the genetic marker M (not indicated). The calculated genomic lengths are shown in kilobases on the right. Bar lengths are not drawn to scale.

strains have been described. Interestingly, all cp CSFV field isolates analyzed so far represent helper virus-dependent subgenomes lacking most of or the entire genomic region encoding the structural proteins as well as N^{pro}, p7, and NS2. To study fundamental aspects of RNA recombination, we recently established a system that allows efficient generation of recombinant pestiviral genomes after transfection of a synthetic, nonreplicatable transcript into cells infected with noncp BVDV (17). Here, we describe successful adaptation of this system for targeted generation of a helper virus-independent cp CSFV. The resulting unique recombinant CP G1 represents the first helper virus-independent cp CSFV strain that emerged by RNA recombination. It contains a large duplication of viral sequences together with cellular ubiquitin-encoding sequences directly upstream of the NS3 gene. CP G1 is capable of inducing a CPE in different cell lines of porcine and bovine origin.

So far, two studies reported on helper virus-independent cp CSFV. First, after introduction of mutations into noncp CSFV strain C, specifically, a change of histidine residue 297 or 346 to lysine, a CPE was observed in SK6 cells (23). The respective amino acids are part of the catalytic center of viral RNase E^{rns}. However, in this study the presence of cp viral subgenomes was not excluded. Furthermore, introduction of corresponding mutations into the genome of another noncp CSFV strain (Alfort/Tübingen) resulted in an attenuated recombinant virus that did not induce a CPE in PK15 cells (38). It thus remains unclear whether the reported CPE actually resulted from the introduced mutations. In the second report, CSFV strains which do not exhibit the exaltation of Newcastle disease virus (END^-) were shown to induce a CPE restricted to certain porcine cell lines, including FS-L3 and CPK-NS (3, 44). This CPE correlated with expression of large amounts of NS3. However, in contrast to CP G1 (Fig. 3) infections with END^- CSFV strains did not lead to formation of plaques being typical for cp pestiviral strains (3).

Under natural conditions, recombinant viral genomes with insertions of cellular sequences originate from at least two recombination events. This explains why the emergence of cp pestiviruses with host-cell-derived insertions represents a rare event. Along the same line, generation of such cp pestiviruses during cell culture passages of noncp pestiviruses was never reported. In contrast, transfection of the synthetic transcript +ubi-Alfort into cells infected with noncp CSFV apparently facilitated the generation of CP G1, because only one recombination event was required. Compared to classical reverse genetic systems based on infectious cDNA clones, a major advantage of the in vivo RNA recombination system described here is the possibility to generate a large number of recombinant viral RNAs which can be simultaneously selected for replication capability and cytopathogenicity (17). This novel approach resulted in the generation of a helper virus-independent cp CSFV strain and will be useful for future studies on replication and RNA recombination of pestiviruses.

For the closely related BVDV, isolation of CP G1-like field isolates carrying duplicated viral sequences together with insertions of cellular mRNA sequences has frequently been reported (4, 9, 12, 21, 32, 34, 41). In contrast, CSFV field strains with duplications and/or insertions of cellular sequences have not been described so far. This interesting observation might be attributed to the fact that a disease syndrome correlated with the appearance of cp pestiviral strains exists only for cattle infected with BVDV. This disease is well known as fatal mucosal disease (MD), which exclusively occurs in cattle persistently infected with a noncp virus after the emergence of an antigenetically closely related cp BVDV. The severe clinical manifestation of MD in cattle allowed isolation and subsequent characterization of many cp BVDV strains. For pigs, however, persistent infections with CSFV usually lead to death within a few weeks after birth.

Cell culture passages of CP G1 rapidly resulted in the emergence of mutants carrying various genomic deletions. Such events have not been reported to occur during cell culture propagation of cp BVDV field strains harboring duplicated viral sequences together with insertions of cellular mRNA sequences. However, for chimeric cp BVDV strains that were generated by reverse genetics and that carry duplicated viral sequences of heterologous origin, genomic deletions resulting in generation of subgenomes and/or noncp viruses were observed during cell culture passages (4, 9). In contrast, a noncp virus did not emerge during cell culture propagation of CP G1. Instead, our analyses revealed that RNA recombination led to the emergence of the shortened genome of CP G2 that completely replaced CP G1 after 10 cell culture passages. Moreover, biologically cloned CP G2 also showed genetic instability after a limited number of cell culture passages. For subgenomes of tombusvirus, it has been postulated that genomes containing sequences dispensable for replication could have disadvantages compared to those without such sequences (51). Accordingly, selection of the considerably enlarged and genetically unstable genomes of CP G1 and CP G2 to shorter and better replicating genomes by stepwise deletion(s) appears likely. Because increased levels of NS3 have been reported to promote replication efficiency of pestiviruses (26), the maintenance of sequences encoding at least one ubiquitin monomer might represent an additional advantage for replication of the CP G2 genome and the subgenomes 1 to 12.

Our findings suggest that CP G1-like CSFV strains may evolve in the field. However, in contrast to MD in cattle, a defined disease associated with the occurrence of cp CSFV is not known. As described here, genetic instability of helper virus-independent cp CSFV strains together with a functional selection for shorter and better replicating genomes might rapidly lead to deletions. Future investigations will show whether genetically stable, helper virus-independent cp CSFV can be obtained. Furthermore, it will be interesting to investigate whether the observed genetic instability of CP G1 and CP G2 during propagation in cell culture can also be observed in the infected animal. Previous studies concerning the virulence of helper virus-dependent cp CSFV subgenomes led to contradictory results (2, 24). It therefore appears worthwhile to investigate the virulence of helper virus-independent cp CSFV.

Our RNA recombination system allowed targeted generation of a helper virus-independent cp CSFV strain. In general, this novel approach is an attractive alternative to classical reverse genetic systems based on infectious cDNA clones, and it represents a useful tool for various applications. Similar systems have been described for Sindbis virus and poliovirus that allowed generation of infectious viruses by recombination between two synthetic replication-incompetent RNA molecules (20, 42). The results of our work demonstrate the applicability

of RNA recombination for the design of plus-strand RNA viruses exhibiting desired phenotypes.

ACKNOWLEDGMENTS

We thank S. Widauer for excellent technical assistance.

A.G. was supported by SFB 535 Invasionsmechanismen und Replikationsstrategien von Krankheitserregern (TP B8 RNA-Rekombination bei Pestiviren) from the Deutsche Forschungsgemeinschaft.

REFERENCES

1. **Aoki, H., K. Ishikawa, Y. Sakoda, H. Sekiguchi, M. Kodama, S. Suzuki, and A. Fukusho.** 2001. Characterization of classical swine fever virus associated with defective interfering particles containing a cytopathogenic subgenomic RNA isolated from wild boar. J. Vet. Med. Sci. **63:**751–758.
2. **Aoki, H., K. Ishikawa, H. Sekiguchi, S. Suzuki, and A. Fukusho.** 2003. Pathogenicity and kinetics of virus propagation in swine infected with the cytopathogenic classical swine fever virus containing defective interfering particles. Arch. Virol. **148:**297–310.
3. **Aoki, H., Y. Sakoda, S. Nakamura, S. Suzuki, and A. Fukusho.** 2004. Cytopathogenicity of classical swine fever viruses that do not show the exaltation of Newcastle disease virus is associated with accumulation of NS3 in serum-free cultured cell lines. J. Vet. Med. Sci. **66:**161–167.
4. **Baroth, M., M. Orlich, H.-J. Thiel, and P. Becher.** 2000. Insertion of cellular NEDD8 coding sequences in a pestivirus. Virology **278:**456–466.
5. **Becher, P., G. Meyers, A. D. Shannon, and H.-J. Thiel.** 1996. Cytopathogenicity of border disease virus is correlated with integration of cellular sequences into the viral genome. J. Virol. **70:**2992–2998.
6. **Becher, P., M. Orlich, M. König, and H.-J. Thiel.** 1999. Nonhomologous RNA recombination in bovine viral diarrhea virus: molecular characterization of a variety of subgenomic RNAs isolated during an outbreak of fatal mucosal disease. J. Virol. **73:**5646–5653.
7. **Becher, P., M. Orlich, and H.-J. Thiel.** 2000. Mutations in the 5′ nontranslated region of bovine viral diarrhea virus result in altered growth characteristics. J. Virol. **74:**7884–7894.
8. **Becher, P., M. Orlich, and H.-J. Thiel.** 1998. Ribosomal S27a-coding sequences upstream of ubiquitin-coding sequences in the genome of a pestivirus. J. Virol. **72:**8697–8704.
9. **Becher, P., M. Orlich, and H.-J. Thiel.** 2001. RNA recombination between persisting pestivirus and a vaccine strain: generation of cytopathogenic virus and induction of lethal disease. J. Virol. **75:**6256–6264.
10. **Becher, P., A. D. Shannon, N. Tautz, and H.-J. Thiel.** 1994. Molecular characterization of border disease virus, a pestivirus from sheep. Virology **198:**542–551.
11. **Becher, P., and H.-J. Thiel.** 2002. Genus *Pestivirus* (*Flaviviridae*), p. 327–331. *In* C. A. Tidona and G. Darai (ed.), The springer index of viruses. Springer-Verlag, Heidelberg, Germany.
12. **Becher, P., H.-J. Thiel, M. Collins, J. Brownlie, and M. Orlich.** 2002. Cellular sequences in pestivirus genomes encoding gamma-aminobutyric acid (A) receptor-associated protein and Golgi-associated ATPase enhancer of 16 kilodaltons. J. Virol. **76:**13069–13076.
13. **Bolin, S. R., A. W. McClurkin, R. C. Cutlip, and M. F. Coria.** 1985. Severe clinical disease induced in cattle persistently infected with noncytopathogenic bovine viral diarrhea virus by superinfection with cytopathogenic bovine viral diarrhea virus. Am. J. Vet. Res. **46:**573–576.
14. **Brownlie, J., M. C. Clarke, and C. J. Howard.** 1984. Experimental production of fatal mucosal disease in cattle. Vet. Rec. **114:**535–536.
15. **de Castro, M. P.** 1973. An infectious agent causing "spontaneous" degeneration of swine cells in vitro. In Vitro **9:**8–16.
16. **Floegel-Niesmann, G., C. Bunzenthal, S. Fischer, and V. Moennig.** 2003. Virulence of recent and former classical swine fever virus isolates evaluated by their clinical and pathological signs. J. Vet. Med. B Infect. Dis. Vet. Public Health **50:**214–220.
17. **Gallei, A., A. Pankraz, H.-J. Thiel, and P. Becher.** 2004. RNA recombination in the absence of viral replication. J. Virol. **78:**6271–6281.
18. **Gillespie, J. H., J. A. Baker, and K. McEntee.** 1960. A cytopathogenic strain of virus diarrhea virus. Cornell Vet. **50:**73–79.
19. **Gillespie, J. H., B. E. Sheffy, and J. A. Baker.** 1960. Propagation of hog cholera virus in tissue culture. Proc. Soc. Exp. Biol. Med. **105:**679–681.
20. **Gmyl, A. P., E. V. Belousov, S. V. Maslova, E. V. Khitrina, A. B. Chetverin, and V. I. Agol.** 1999. Nonreplicative RNA recombination in poliovirus. J. Virol. **73:**8958–8965.
21. **Greiser-Wilke, I., L. Haas, K. Dittmar, B. Liess, and V. Moennig.** 1993. RNA insertions and gene duplications in the nonstructural protein p125 of pestivirus strains and isolates in vitro and in vivo. Virology **193:**977–980.
22. **Heinz, F. X., M. S. Collett, R. H. Purcell, E. A. Gould, C. R. Howard, M. Houghton, R. J. M. Moormann, C. M. Rice, and H.-J. Thiel.** 2000. Family Flaviviridae, p. 859–878. *In* C. M. Fauquet, M. H. V. van Regenmortel, D. H. L. Bishop, E. B. Carstens, M. K. Estes, S. M. Lemon, J. Maniloff, M. A. Mayo, D. J. McGeoch, C. R. Pringle, and R. B. Wickner (ed.), Virus taxonomy: seventh report of the International Committee on Taxonomy of Viruses. Academic Press, Inc., San Diego, Calif.
23. **Hulst, M. M., F. E. Panoto, A. Hoekman, G. P. van Gennip, and R. J. M. Moormann.** 1998. Inactivation of the RNase activity of glycoprotein E^{rns} of classical swine fever virus results in a cytopathogenic virus. J. Virol. **72:**151–157.
24. **Kosmidou, A., M. Büttner, and G. Meyers.** 1998. Isolation and characterization of cytopathogenic classical swine fever virus (CSFV). Arch. Virol. **143:**1295–1309.
25. **Kümmerer, B. M., and G. Meyers.** 2000. Correlation between point mutations in NS2 and the viability and cytopathogenicity of bovine viral diarrhea virus strain Oregon analyzed with an infectious cDNA clone. J. Virol. **74:**390–400.
26. **Lackner, T., A. Müller, A. Pankraz, P. Becher, H.-J. Thiel, A. E. Gorbalenya, and N. Tautz.** 2004. Temporal modulation of an autoprotease is crucial for replication and pathogenicity of an RNA virus. J. Virol. **78:**10765–10775.
27. **Laude, H.** 1978. Isolation of a cytolytic strain of hog cholera virus from IB-RS2 cells. Ann. Microbiol. (Paris) **129:**553–561. (In French.)
28. **Lee, K. M., and J. H. Gillespie.** 1957. Propagation of virus diarrhea virus of cattle in tissue culture. Am. J. Vet. Res. **18:**953.
29. **Lindenbach, B. D., and C. M. Rice.** 2001. Flaviviridae: the viruses and their replication, p. 991–1041. *In* D. M. Knipe and P. M. Howley (ed.), Fields Virology, 4th ed., vol. 1. Lippincott Williams & Wilkins, Philadelphia, Pa.
30. **Meyers, G., T. Rümenapf, and H.-J. Thiel.** 1989. Molecular cloning and nucleotide sequence of the genome of hog cholera virus. Virology **171:**555–567.
31. **Meyers, G., T. Rümenapf, and H.-J. Thiel.** 1989. Ubiquitin in a togavirus. Nature **341:**491.
32. **Meyers, G., D. Stoll, and M. Gunn.** 1998. Insertion of a sequence encoding light chain 3 of microtubule-associated proteins 1A and 1B in a pestivirus genome: connection with virus cytopathogenicity and induction of lethal disease in cattle. J. Virol. **72:**4139–4148.
33. **Meyers, G., N. Tautz, P. Becher, H.-J. Thiel, and B. Kümmerer.** 1996. Recovery of cytopathogenic and noncytopathogenic bovine viral diarrhea viruses from cDNA constructs. J. Virol. **70:**8606–8613.
34. **Meyers, G., N. Tautz, E. J. Dubovi, and H.-J. Thiel.** 1991. Viral cytopathogenicity correlated with integration of ubiquitin-coding sequences. Virology **180:**602–616.
35. **Meyers, G., and H.-J. Thiel.** 1995. Cytopathogenicity of classical swine fever virus caused by defective interfering particles. J. Virol. **69:**3683–3689.
36. **Meyers, G., and H.-J. Thiel.** 1996. Molecular characterization of pestiviruses. Adv. Virus Res. **47:**53–118.
37. **Meyers, G., H.-J. Thiel, and T. Rümenapf.** 1996. Classical swine fever virus: recovery of infectious viruses from cDNA constructs and generation of recombinant cytopathogenic defective interfering particles. J. Virol. **70:**1588–1595.
38. **Meyers, M., A. Saalmüller, and M. Büttner.** 1999. Mutations abrogating the RNase activity in glycoprotein E(rns) of the pestivirus classical swine fever virus lead to virus attenuation. J. Virol. **73:**10224–10235.
39. **Mittelholzer, C., C. Moser, J.-D. Tratschin, and M. A. Hofmann.** 1997. Generation of cytopathogenic subgenomic RNA of classical swine fever virus in persistently infected porcine cell lines. Virus Res. **51:**125–137.
40. **Moser, C., P. Stettler, J.-D. Tratschin, and M. A. Hofmann.** 1999. Cytopathogenic and noncytopathogenic RNA replicons of classical swine fever virus. J. Virol. **73:**7787–7794.
41. **Qi, F., J. F. Ridpath, and E. S. Berry.** 1998. Insertion of a bovine *SMT*3B gene in NS4B and duplication of NS3 in a bovine viral diarrhea virus genome correlate with the cytopathogenicity of the virus. Virus Res. **57:**1–9.
42. **Raju, R., S. V. Subramaniam, and M. Hajjou.** 1995. Genesis of Sindbis virus by in vivo recombination of nonreplicative precursors. J. Virol. **69:**7391–7401.
43. **Roehe, P. M., and S. Edwards.** 1994. Comparison of pestivirus multiplication in cells of different species. Res. Vet. Sci. **57:**210–214.
44. **Sakoda, Y., M. Hikawa, T. Tamura, and A. Fukusho.** 1998. Establishment of a serum-free culture cell line, CPK-NS, which is useful for assays of classical swine fever virus. J. Virol. Methods **75:**59–68.
45. **Schägger, H., and G. von Jagow.** 1987. Tricine-sodium dodecyl sulfate-polyacrylamide gel electrophoresis for the separation of proteins in the range from 1 to 100 kDa. Anal. Biochem. **166:**368–379.
46. **Tautz, N., G. Meyers, and H.-J. Thiel.** 1993. Processing of poly-ubiquitin in the polyprotein of an RNA virus. Virology **197:**74–85.
47. **Tautz, N., H.-J. Thiel, E. J. Dubovi, and G. Meyers.** 1994. Pathogenesis of mucosal disease: a cytopathogenic pestivirus generated by internal deletion. J. Virol. **68:**3289–3297.
48. **Thiel, H.-J., P. G. W. Plagemann, and V. Moennig.** 1996. Pestiviruses, p. 1059–1073. *In* B. N. Fields, Knipe, D. M. and P. M. Howley (ed.), Fields Virology, 3rd ed., vol. 1. Lippincott-Raven Publishers, Philadelphia, Pa.
49. **van Bekkum, J. G., and S. J. Barteling.** 1970. Plaque production by hog cholera virus. Arch. Gesamte Virusforsch. **32:**185–200.
50. **Weiland, E., R. Ahl, R. Stark, F. Weiland, and H.-J. Thiel.** 1992. A second envelope glycoprotein mediates neutralization of a pestivirus, hog cholera virus. J. Virol. **66:**3677–3682.
51. **White, K. A., and T. J. Morris.** 1994. Nonhomologous RNA recombination in tombusvirus: generation and evolution of defective interfering RNAs by stepwise deletions. J. Virol. **68:**14–24.